LA-UR-85-2821
CONF-850770--9

SEP 1 0 1985

Los Alamos National Laboratory is operated by the University of California for the United States Department of Energy under contract W-7405-ENG-36

LA-UR--85-2821

DE85 017567

TITLE TEMPERATURE KINETICS DURING SHOCK-WAVE CONSOLIDATION OF METALLIC POWDERS

AUTHOR(S) R. B. Schwarz, CMS
P. Kasiraj, IBM San Jose Research Laboratory
T. Vreeland, Jr., California Institute of Technology

SUBMITTED TO Presented at the International Conference on Metallurgical Applications of Shock-Wave and High Strain Rate Phenomena

DISCLAIMER

Los Alamos National Laboratory
Los Alamos, New Mexico 87545

TEMPERATURE KINETICS DURING SHOCK-WAVE CONSOLIDATION OF METALLIC POWDERS

R. B. SCHWARZ, P. KASIRAJ, and T. VREELAND, Jr.

Center for Materials Science
Los Alamos National Laboratory
Los Alamos, NM 87545

IBM San Jose Research Laboratory
San Jose, CA 95193

California Institute of Technology
Pasadena, CA 911225

Powders (60 μm diam) of constantan and pure copper were compressed statically into cylindrical greens (20.3 mm diam, 5.3 mm long) with a flat interface separating the two powders. A 20-mm propellant gun was used to accelerate a flyer of Lexan, copper, or aluminum, and generate in the green a shock wave with front parallel to the Cu/constantan interface. The voltages between opposite ends of the greens were measured as a function of time and for shock pressures between 1.3 and 9.4 GPa. When the shock wave arrives at the Cu/constantan interface, the voltage signal shows an abrupt increase, which lasts between 45 and 81 ns and leads to a peak temperature T_p. After this, the hotter and cooler parts of the compact equilibrate and the temperature decreases to a value T_h. With increasing shock pressure, T_h increases from 425 to 1215 K. The measurements of T_h are in excellent agreement with the temperatures calculated from the measured flyer velocity, the Hugoniot for copper powder, and thermodynamic data for the flyer and powders.

1. INTRODUCTION

The propagation of a shock wave through a porous material is a highly non-conservative process, since significant energy is dissipated during the shock rise time. For shock waves of sufficient strength, the powder reaches the bulk density by the end of the shock rise time . Because the rise times are typically 40-80 ns, the plastic strain rate near the material surrounding the original cavities can be as high as 10^7 s^{-1}. For optimum shock parameters, the heavily deformed material melts, while the less deformed material (away from the cavities) reaches a much lower temperature. Furthermore, because the material velocity in the shocked powder is not constant, friction between powder particles is thought to raise the temperature of the particle surfaces. Evidence of local melting along particle boundaries and at sites of pore coalescence have been provided on the basis of metallographic analyses of the compacts [1-3]. The subsequent quenching of the melt pools by heat conduction into the less deformed regions lasts approximately $t_h = d^2/4D$, where d is the particle diameter and D is the thermal diffusivity. Typically, $t_h \approx 200$ ns [4]. Thus, for internal temperature differences of a few hundred Kelvin, the melt pools cool at rates of the order of 10^9 K/s. For the appropiate alloys, this quenching is sufficiently fast to solidify the melt into metastable structures. Indeed, shock waves have been used to consolidate amorphous powders [5] and rapidly solidified powders [6-8] without an appreciable change in their microstructures.

Several models and calculations have been recently advanced [3,4,6,9] to describe the dynamic events occurring during the shock consolidation of powders. The evaluation of these models requires accurate measurements of the temperature kinetics during shock consolidation. Starting with the work of Jacquesson [10] in 1959, several efforts have been made to measure the temperature rise behind a shock front using thermocouples. However, in the early experiments, the temperatures deduced from the measured emf were twofold to threefold larger than those inferred from measured shock parameters. It has recently become clear that the anomalously large signals were due to experimental artifacts. Bloomquist and coworkers [11,12] reviewed the literature and performed experiments using diffusion-bonded metallic pairs. In these carefully-controlled experiments, the measured emf was within 20% of the predicted value.

An important source of error in the early thermocouple experiments was friction between the two metals forming the thermocouple, or between the thermocouple and the medium in which these were imbedded. It is easy to realize that if the thermocouple and the medium have different Hugoniots, the shock wave will accelerate them to different particle velocities. Friction between these parts will increase the temperature of the thermocouple above that in the rest of the medium and thus give an excessive signal. This deleterious effect is more pronounced in porous media. Therefore, wire or thin foil thermocouples imbeded in powders cannot be expected to yield reliable shock temperatures. On the other hand, it has been shown by Nesterenko [13], that meaningfull emf signals can be obtained with thermocouples formed by two metallic powders. The method requires that the interface between the powders be parallel to the shock front and that the two powders be of similar densities and size distribution, but of different thermoelectric powers. In Nesterenko's experiments the thermocouple was made from powders of copper and nickel with particle sizes between 0.1 and 1 mm. These were shocked to pressures between 0.9 and 2.5 GPa.

In the present experiments the thermocouple was formed by powders of copper and constantan with particle sizes between 30 and 100 μm. These were shocked to pressures between 1.3 and 9.4 GPa. Copper and constantan were chosen because: (a) these metals have a large difference in absolute thermopower, (b) neither of the powders is magnetic, (c) the pressure correction to the thermal emf of copper and constantan has been measured [14,15] and (d) the shock impedances of copper and constantan are almost identical for the pressure range of interest [11].

II. SYNTHESIS OF CONSTANTAN POWDER AND THERMOCOUPLE CALIBRATION

Since powder of constantan could not be obtained commercially, we synthesized it by mechanical alloying. The starting materials were 55% copper powder and 45% nickel powder, by weight (Alfa Products #00094 and #00665, respectively). The mechanical alloying (MA) was done in a SPEX mixer 8000 model, as described elsewhere [16]. Following 5 hr of MA, the powder was further homogenized by anneal in purified hydrogen at 750°C for 16 hr. The powder was finally ground to -200 mesh in a SPEX shatterbox model 8500 using a hardened-steel dish and peg which were pre-cooled to 78K. The final product was dried in a N_2 atomosphere.

Figure 1 shows the (111), (200), and (220) X-ray diffraction peaks (Cu K-α radiation) as a function of MA time. The lattice constant of the MA constantan powder is $a_{Cn} = 3.55 \pm 0.01$ Å which is somewhat lower than the value 3.57 Å deduced from Vagard's law. This difference is to be expected [17].

Because the present constantan powder may contain iron impurities introduced during MA, or have a composition slightly different from that of the commercial product, the thermal emf of our copper/constantan thermocouple may differ from that tabulated in handbooks of physics. The calibration of the porous thermocouple was performed with 45-cm long, 1.5-mm diameter rods of constantan and copper sintered from the same powders used in the shock experiments. The reference temperature was measured with Pt/Pt-10% Rh thermocouples which were themselves calibrated at the solidification temperature of high-purity silver. The measured emf-vs-T curve covers the range 0-955°C. At 400°C, the emf of the present powder thermocouple exceeds that of commercial thermocouples by 11.4%.

III. EXPERIMENTAL SETUP

The shock compaction experiments were performed with the 20-mm diameter gun of the Seismological Laboratory at the California Institute of Technology. Two laser beams located near the end of the gun were used to measure the flyer velocity.

Figure 2 is a schematic cross-sectional view of the shock assembly. The figure shows a flyer and plastic sabot after leaving the gun and before impacting on the copper buffer plate. The statically-compacted powder, or 'green', was fabricated by pressing various layers of copper, constantan, and alumina powders carefully assembled inside a cylindrical die. The die diameter was 20.3 mm and the final pressure 140 GPa, giving a green density of 5.27 g/cm^3. A quartz tube (8 mm long, 14 mm OD, and 11.7 mm ID) was imbedded in the powder, separating the copper and constantan powders. The copper/constantan junction is inside this tube and is parallel to the copper buffer plate. The active diameter of the thermocouple junction was further reduced to 4.7 mm by the addition of a thin ring of alumina powder (not shown in Fig. 2). This was done to avoid spurious effects from the shock reflections at the powder/quartz interface and to minimize the effects of tilt between the shock wave front and the copper/constantan interface. Copper powder was added behind the constantan powder to facilitate the soldering of the coaxial cable that transmits the signal to

the oscilloscope. This creates a second constantan/copper junction which does not affect the measurements until the much later arrival of the shock wave to that junction. The green is in vacuum and is held against the copper buffer plate with a few drops of epoxy cement placed on its outer cylindrical surface.

The internal impedance of the powder thermocouple was less than 0.1 ohm. Since the coaxial cable was terminated at the oscilloscope by its characteristic impedance of 50 ohm, the measured signal was approximately equal to the thermal emf. For further experimental details see Ref.[18].

IV. CALCULATED SHOCK PRESSURE, ENERGY DISSIPATION, AND HOMOGENEOUS TEMPERATURE

Flyers made of Lexan, 2024 aluminum, and copper were accelerated to speeds of 1 to 1.5 km/s. The shock pressure was calculated by the matching-shock-impedance method. The Hugoniots for solid copper and aluminum were taken from Ref.[19]. A smooth Hugoniot for copper powder was obtained from an analytical equation for porous media [21] which was fitted to the data in Ref.[20]. The shock states calculated by this method assume one-dimensional flow conditions. Since the flyer has a finite diameter, conical pressure release waves propagate into the buffer plate and later into the green. The dimensions of the shock assembly in Fig. 2 were chosen so that the lateral pressure release waves reach the constantan powder at a point behind the copper/constantan junction.

For powders, the total energy dissipated by the shock wave largely exceeds that which is stored internally as defects, etc. Thus, to a good approximation, the energy dissipated as heat is given by

$$E = PV_0(V_{00}/V_0 - 1)/2 \qquad (1)$$

where V_0 and V_{00} are the specific volumes (m^3/kg) of the solid and powder, respectively. For the present greens, $V_{00}/V_0 = 1.67$. Table 1 contains the calculated shock pressures and shock energies for the four tests performed.

The shock energy E is dissipated preferentially near particle boundaries and cavities in the green. However, after a time t_h (of the order of 200 ns [4]), the compact reaches a homogeneous temperature, T_h. In what follows we calculate T_h in copper and in constantan as a function of shock energy dissipation, E. In sections 5 and 6 we compare these values

with those deduced from the measured emf. Neglecting the difference between c_p and c_v, T_h is given by the implicit equation,

$$\int_{T_0}^{T_h} c_p dT = E \qquad (2)$$

where T_0 is the initial (ambient) temperature.

In the temperature range $400 < T < 1200$ K, the specific heats at constant pressure, c_p, and thermal conductivities, K, of copper and constantan are satisfactorily described by the relationships [22]

$$c_{p,cu}\ (\text{cal/g·K}) = 0.085 + 2.4 \times 10^{-5}\ T(\text{K}) \qquad (3a)$$

$$c_{p,cn}\ (\text{cal/g·K}) = 0.087 + 3.7 \times 10^{-5}\ T(\text{K}) \qquad (3b)$$

$$K_{cu}\ (\text{cal/s·cm·K}) = 1.02 - 2.1 \times 10^{-4}\ T(\text{K}) \qquad (4a)$$

$$K_{cn}\ (\text{cal/s·cm·K}) = 0.02 + 8.0 \times 10^{-5}\ T(\text{K}) \qquad (4b)$$

where the sub-index cn denotes constantan. For a given shock energy dissipation E, the homogeneous temperatures $T_{h,cu}$ and $T_{h,cn}$ were calculated from equations (2)-(4). Because $c_{p,cn}$ is slightly larger than $c_{p,cu}$, $T_{h,cu}$ is approximately 6% larger than $T_{h,cn}$. However, the Cu/constantan junction assumes a temperature T_j that is independent of time and is given by [23].

$$T_j = T_{h,cn} - (T_{h,cu} - T_{h,cn})/(\beta - 1) \qquad (5)$$

where $\beta = (K_{cu}/K_{cn})(D_{cn}/D_{cu})^{1/2}$ and D is the thermal diffusivity. The curve in Fig. 3 shows the calculated T_j as a function of shock energy dissipation, E.

V. TEMPERATURE MEASUREMENTS

Figure 4 shows the time dependence of the thermal emf for run # 798, photographed from the oscilloscope screen. The traces for the other three experiments are almost identical in shape. Figure 5 is a schematic of Fig. 4, which defines characteristic temperatures and time constants. The oscilloscope is triggered by the shorting of the thin enamel-coated wire placed in front of the buffer plate (Fig. 2). During the time the shock wave is traversing the buffer plate and copper powder, the emf signal is zero. Because the copper powder is at ground potential, a negative pulse

appears when the shock front arrives at the thermocouple junction. The emf signal raises to a peak value V_p in time t_1. It then decays with time constant t_2, to a value V_h. A careful examination of Fig. 4 shows that V_h also decays in time but at a much slower rate.

Table 2 summarizes the emf measurements, the junction temperatures, and the characteristic times deduced from these measurements. A direct emf-to-temperature conversion using the calibration curve described in Section 4 gives the T'_h values in column 2 of Table 2. These values must be corrected for the pressure dependence of the emf. This correction has been described in detail in Ref. [11]. From equation (5b) in that work it follows that at a pressure P and temperature T the measured emf is lower than that at P = 0 by an amount

$$\Delta V(\mu V) = 0.14 \cdot P(GPa) \cdot T(K) \qquad (6)$$

The pressure correction to the measured emf is given in column 4 of Table 2. Column 5 in this table has the corrected T_h values. The four data points in Fig. 3 were plotted with the data in column 5 of Tables 1 and 2.

VI. DISCUSSION

Variables in the shock consolidation of powders are the shock energy dissipation E (proportional to the shock pressure P), and the duration of the shocked state, t_d. A model was recently advanced [4] which predicts the regimes of E and t_d for the optimum consolidation of powders. The model is based on an analysis of the consolidation process in terms of discrete physical processes, each characterized by a time constant. These are: (a) densification of the powder to the bulk density and melting of material in the proximity of interparticle boundaries (time constant t_r), (b) solidification of the melt pockets (time constant t_s), (c) thermal relaxation within the shocked material to a homogeneous temperature T_h (time constant t_h), and (d) thermal relaxation of the compact to ambient temperature (time constant t_a). The present measurements support this model, as will be discussed next.

Following the arrival of the shock front at the copper/constantan interface, the emf signal increases rapidly to a peak value V_p. The measured rise time, t_1, is between 45 and 81 ns. Preliminary measurements using thin film thermocouples [23] gave t_r = 40 ns. Because the tilt

between the flyer and buffer plate at impact can reach values of up to one degree [18], the t_1 measurements are most likely an upper limit for the actual temperature rise-time at the copper/constantan interfaces. Thus, an upper limit for the width of the shock front is $w = v_s \cdot t_1$, where v_s is the shock velocity in the powder. Using the averages of the values in column 4 of Table 1 and column 6 in Table 2 we obtain $w \approx 90$ μm. This width is within a factor of 2 from the diameter of the copper powder (40 to 70 μm) or the constantan power (30 to 90 μm). The width of a shock front in powders has been estimated [6] to be 3.6 times the particle diameter. The present measurements give a somewhat lower value.

The peak voltage signal, V_p, is reached near the completion of the densification of the powder. At this point the temperature in the compact is heterogeneous, with the material originally surrounding voids and particle boundaries being hotter than the particle interiors. However, since not all the copper/constantan particle boundaries reach the same temperature, V_p cannot be easily interpreted. If we assume that all the particle boundaries have the same electrical impedance, then V_p gives the average of the distribution of emf from the different copper/constantan interfaces.

Following the peak value, the emf signal decreases quasi-exponentially with time constant t_2 to a value V_h. In what follows we use the numerical value of t_2, as well as the observation that $t_2 \gg t_1$, to infer about the temperature distribution in the powder at the end of the densification process.

Several authors [4,6,9] have assumed that the shock energy E dissipated during the rise time is deposited at the particle surfaces. It is easy to show that if this is the case, the relaxation time for the cooling of the heated surface must be approximately equal to the shock rise time. Consider, for example, a semi-infinite solid at temperature T_0 that is irradiated for a time interval t_1 by a heat flux F_0. The temperature of the irradiated surface is given by [24]

$$T = T_0 + At^{1/2} \qquad 0 < t < t_1 \qquad (7)$$

$$T = T_0 + A[t^{1/2} - (t-t_1)^{1/2}] \qquad t > t_1 \qquad (8)$$

where $A = (2F_0/K)(D/\pi)^{1/2}$. Thus, the initial rates of heating and cooling at the particle surfaces are equal. The same conclusion follows

from Fig. 10 in Ref. [9], which shows the numerical calculations of Gourdin (1984) for the surface temperature of a uniform sphere irradiated for a finite time by a constant heat flux F_0. Both examples are in conflict with the present measurement, which show that the initial cooling rate largely exceeds the heating rate (i.e., $t_2 >> t_1$; see Figs. 4 and 5). The discrepancy arises from the assumption made in the the models that the shock energy is dissipated at the surface of the particles. In what follows we assume a more realistic model in which the shock energy is dissipated in a band of thickness Δx surrounding the original powder particles. We further simplify the model by assuming a one-dimensional temperature distribution, as shown in Fig. 6. At $t = t_1$ the hot regions are at temperature T_p and have a thickness Δx. We further assume that the shocked material is solid and homogenous (no melt present), and that the thermal properties (specific heat, thermal conductivity) are constant. The temperature distribution during cooling, $T(x,t)$, has been deduced [23] in the form of a series expansion. For $x = 0$ it reduces to:

$$T(0,t') = T_h + \frac{2}{d} \sum_{n=1}^{\infty} a_n \exp(-D\, n^2\pi^2 t'/d^2) \qquad (9)$$

where $t' = t - t_1$, T_h is the homogeneous temperature for $t \to \infty$, and

$$a_n = \int_0^d T(x',0) \cos \frac{n\pi x'}{d}\, dx'. \qquad (10)$$

From symmetry considerations, $a_n = 0$ for $n =$ odd. Furthermore, from equation (10) and Fig. 6 it is easy to realize that the coefficients a_n have approximately the same value as long as $n < d/\Delta x$, but decrease as $1/n$ for larger values of n. Thus, the initial decay in $T(0,t')$ is primarily determined by the exponential term in equation (9) with $n = d/\Delta x$. Using this value of n, and equating the decay time constant in equation (9) with the measured decay time t_2, we obtain $\Delta x = \Pi(Dt_2)^{1/2}$. With $t_2 = 200$ ns and $D = 0.5$ cm^2/s (average of the ther-mal diffusivities of copper and constantan in the regime $400 < T < 1000$ K), we obtain $\Delta x = 10\mu$m.

The above results have a further implication. Because the shock energy E is dissipated within a skin of thickness $\Delta x/2$ surrounding each particle, the onset of interparticle melting requires a critical shock energy E_c. For spherical particles, $E_c/H_m = 3\Delta x/d$, where H_m is the heat of fusion. For the present powders with $d = 60$ μm and the estimate

Δx = 10 μm, $E_c/H_m \approx 0.5$. Measurements of melt fractions as a function of shock pressure [2,9] and of shock energy ([18]; Vreeland and coworkers, this conference) show the existence of E_c. The later measurements in Marko-1064 alloy ($Ni_{52.5}Mo_{38}Cr_8B_{1.5}$) give $E_c/H_m \approx 0.3$.

The present tests do not discern whether there is interparticle melting. Recovery experiments by Morris in tool steel powder ([2]; see also discussion in Ref. [4]) show that interparticle melting occurs for shock energies in excess of 380 J/g. Because copper has a larger thermal diffusivity than steel, it is unlikely that interparticle melting took place in the first three tests in Tables 1 and 2. However, the emf vs. time record for Test 802, with shock energy E = 363 J/g, shows a cooling time constant, t_2 = 630 μs, which is significantly larger than that for the tests at the lower shock energies. This increase in thermal relaxation time is suggestive of the formation of melt pools.

The present measurements of t_1 and t_2 at the copper/constantan interfaces can be compared with the time constants t_r and t_h calculated in Ref. [4] for iron-based powders . This shows that $t_1 \approx t_r \approx 40$ ns. The relaxation time for reaching a homogeneous temperature near the Cu/constantan interfaces is roughly $3 \cdot t_2 \approx 0.6$ ms. On the other hand, for the Fe-based powder, t_r = 10 ms. This difference is explained by the smaller thermal diffusivity of Fe, by a factor of 10.

VII. CONCLUSIONS

The temperature kinetics at the boundary of powder particles of copper and constantan has been measured during shock consolidation using the powder itself as a thermocouple. We conclude that:

(1) The initial rise time in temperature lasts between 45 and 80 ns. From this it follows that the width of the shock front is approximately equal to the particle size.

(2) The peak temperature largely exceeds the homogeneous temperature of the thermally relaxed compact, showing that during densification most of the shock energy is deposited near interparticle boundaries.

(3) The time constant for the thermal relaxation of the compact to the homogeneous temperature T_h is significantly longer than the shock rise time. This means that the shock energy is not deposited at the particle surfaces, as previously assumed, but within regions of finite width. Assuming these regions surround the powder particles, we estimate their width to be 14 μm.

(4) The measured homogeneous temperature is in excellent agreement with the temperature calculated using the measured flyer velocity, density of the powder, published Hugoniots for copper powder, and themodynamic data. This agreement gives confidence on the assumptions usually made for the analytical treatment of shock waves in powders. In particular, it shows that the deformation front in a metallic powder is indeed a steady-state one-dimensional shock front.

Acknowledgements: The authors thank Professor T.J. Ahrens for the use of the 20 mm gun. Research supported by United Technologies Research Center and Defense Advanced Projects Agency through the U.S. Army Materials and Mechanics Research Center, and by the U.S. Department of Energy.

REFERENCES

1. D. Raybould, J. Materials Sci. 16, 589 (1981).
2. D. G. Morris, Metal Science 15, 116 (1981).
3. A. M. Staver, in "Shock Waves and High Strain Rate Phenomena in Metals" (edited by M. A. Mayers and L. E. Murr), p. 865. Plenum Press, New York (1981).
4. R. B. Schwarz, P. Kasiraj, T. Vreeland Jr., and T.J. Ahrens, Acta Metall. 32, 1243 (1984).
5. C. F. Cline and R. W. Hopper, Scripta Metall. 11, 1137 (1977).
6. D. Raybould, Int. J. Powder Metall. Powder Tech. 16, 9 (1980).
7. M. A. Meyers, B. B. Gupta, and L. E. Murr, J. of Metals 33, 21 (1981).
8. P. Kasiraj, T. Vreeland Jr., R. B. Schwarz, and T. J. Ahrens, Acta Metall. 32, 1235 (1984).
9. W. H. Gourdin, J. Appl. Phys. 55, 172 (1984).
10. J. Jacquesson, Bull. du G.A.M.A.C. IV, 4, 33 (1959).
11. D. D. Bloomquist, G. E. Duvall, and J. J. Dick, Washington State University Report F49620-77-C-0034, 1978.
12. D. D. Bloomquist, Thesis, Washington State University (1978).
13. V. F. Nesterenko, Paper presented at the All-Union School on Explosion Physics in Krasnoyarsk, USSR (1984). English translation by the Berkeley Scientific Transl. Service, #UCRL-TRANS-12054, March 1985.
14. P.W. Bridgman, Proc. Am. Acad. Arts Sci. 53, 269 (1918).
15. F. P. Bundy, J. Appl. Phys. 32, 483 (1961).
16. R. B. Schwarz, R. R. Petrich, and C. K. Saw, J. non Cryst. Solids, (in print, 1985).

17. T. B. Massalski in "Physical Metallurgy" (edited by R. W. Cahn and P. Haasen), part 2, p. 153. North Holland Press, Amsterdam (1983).
18. P. Kasiraj, Thesis, California Institute of Technology (1985).
19. R. G. McQueen, S. P. Marsh, J. W. Taylor, J. N. Fritz, and W. J. Carter, in "High Velocity Impact Phenomena" (edited by R. Kinslow), p. 293. Academic Press, New York (1970).
20. R. R. Boade, J. Appl. Phys. 39, 5693 (1968).
21. G. A. Simons and H. H. Legner, J. Appl. Phys. 53, 934 (1982).
22. Y. S. Toulokian, R. W. Powell, C. Y. Ho and P. G. Klemens, "Thermophysical Properties of Matter," Plenum Press, New York (1970).
23. R. B. Schwarz, P. Kasiraj, T. Vreeland Jr. and T. J. Ahrens, Bull. Am. Phys. Soc. 28, 460 (1983).
24. H. S. Carslaw and J. C. Jaeger, "Conduction of Heat in Solids," Oxford University Press (1959).

TABLE 1 Shock parameters for tests in porous copper/constantan thermocouples.

Test #	Flyer Material	Measured	Calculated		
		Flyer Velocity (km/s)	Shock Velocity in Cu powder (km/s)	Shock Pressure (GPa)	Shock Energy (J/g)
801	Lexan	1.49	0.75	1.3	50
		±0.05	±0.06	±0.2	±9
798	2024 Al	1.03	1.23	3.5	135
800	2024 Al	1.39	1.63	6.0	232
802	Cu	1.13	2.03	9.4	363

Table 2 Homogeneous temperature and time constants deduced from the emf versus time records.

Test #	Measured emf	T_h'	Pressure Correction to emf	T_h	Measured	
					t_1	t_2
	(mV)	(K)	(mV)	(K)	(ns)	(ns)
801	-6.5±1.5	403±30	0.073	410±30	67±13	140±30
798	-20.0	626	0.31	631	81±13	220±30
800	-38.0	877	0.74	890	45±12	200±20
802	-58.4	1148	1.51	1165	63±31	630±60

FIG. 1 X-ray diffraction intensity (Copper K-α radiation of a mechanically alloyed mixture of 55% copper and 45% nickel powders. (a) After mechanical alloying (MA) for 10 min; (b) after MA for 3.5 hr; (c) after MA for 5 hr and a thermal anneal in purified hydrogen at 750°C for 16 hrs.

FIG. 2 Schematic cross-sectional view of the projectile and shock assembly.

FIG. 3 The curve gives the calculated homogeneous temperature at the interface between the compacted copper and constantan powders as a function of shock energy. The dots are the measured homogeneous temperatures in shock experiments at four differnt shock energies.

FIG. 4 Photograph of the oscilloscope trace of the emf signal for test #798. Vertial scale: 20 mV/div. Horizontal scale: 0.5 μs/div.

FIG. 5 Schematic of the trace in Fig. 4, defining the voltage signals V_p and V_h, and the time parameters t_1 and t_2.

FIG. 6 One-dimensional model for the temperature distribution at the beginning of the snocked state (end of the shock rise time).

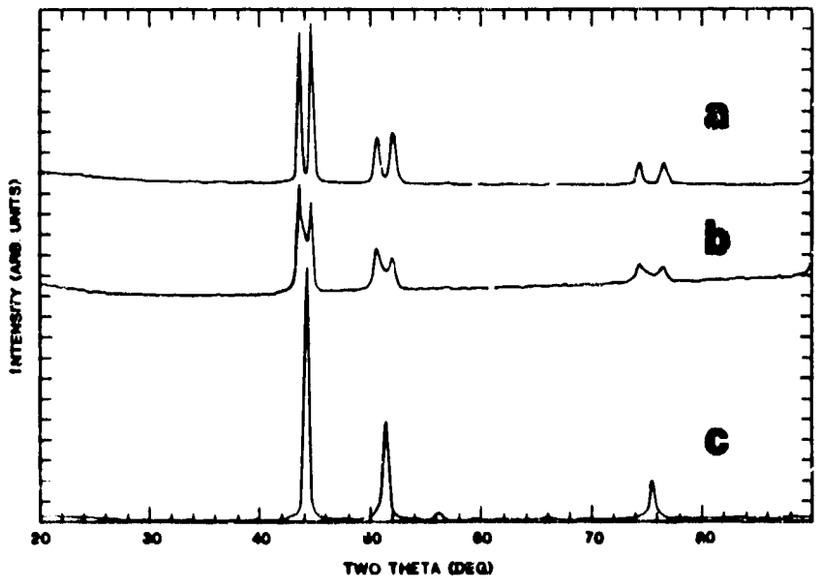
a
b
c
INTENSITY (ARB UNITS)
20
30
40
50
60
70
80
TWO THETA (DEG)

Fig. 1

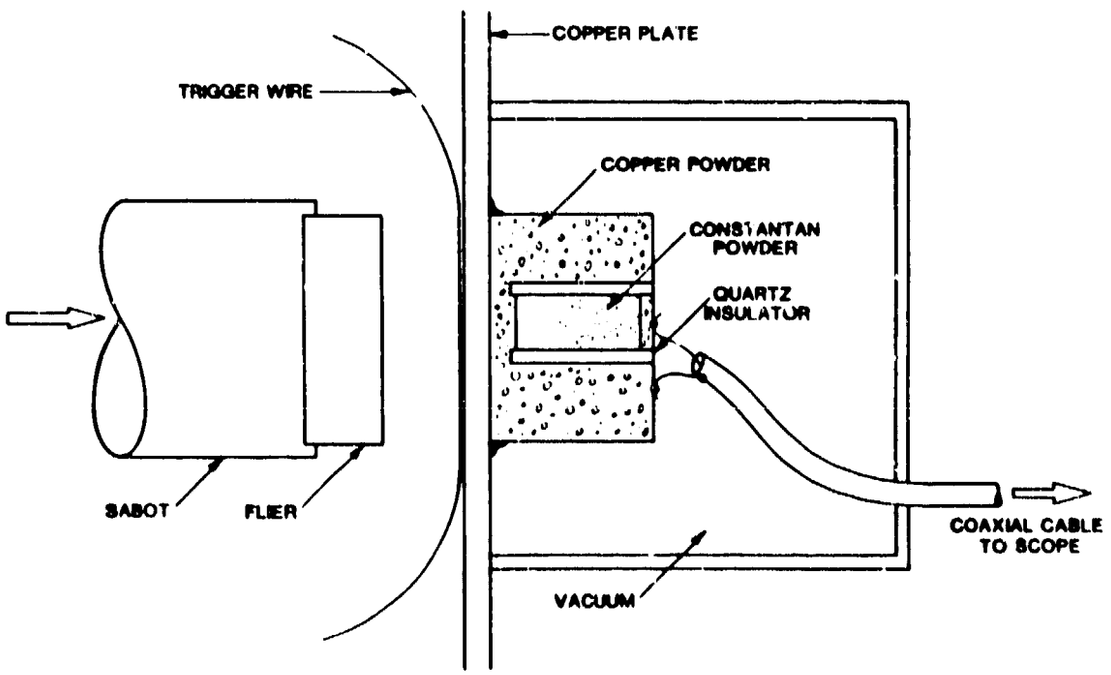
COPPER PLATE
TRIGGER WIRE
COPPER POWDER
CONSTANTAN POWDER
QUARTZ INSULATOR
SABOT
FLIER
COAXIAL CABLE TO SCOPE
VACUUM

Fig. 2

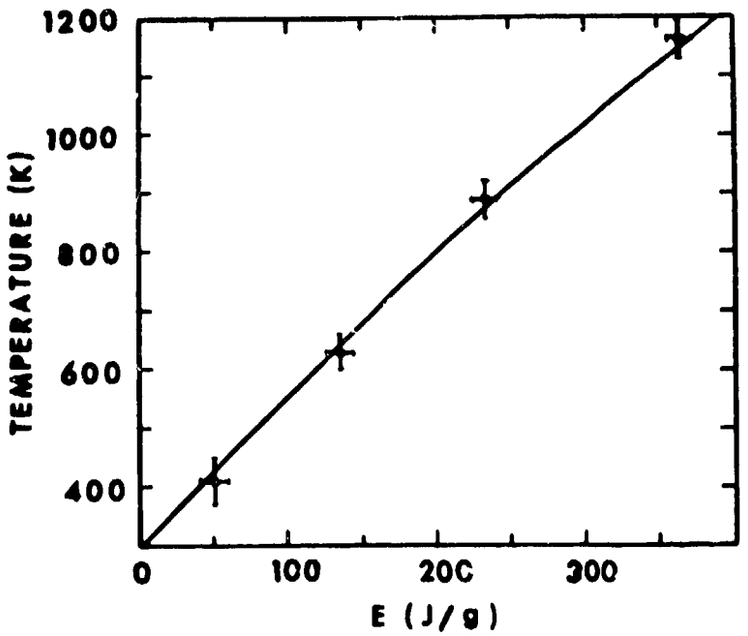

Fig. 3

Fig. 4

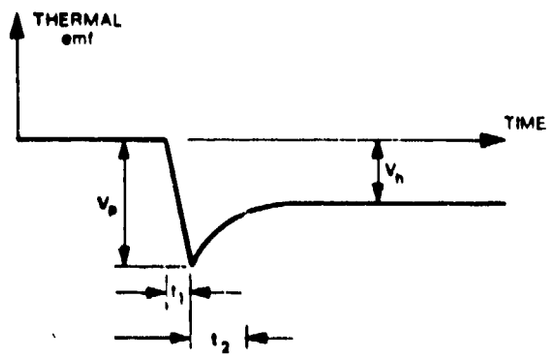

Fig. 5

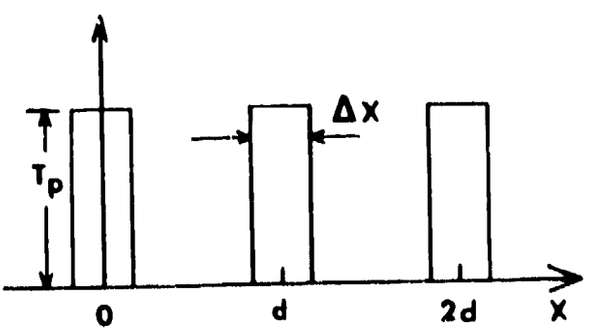

Fig. 6